MODERN MEDICINE AND PRACTICE
https://inovatus.es/index.php/ejmmp
EUROPEAN JOURNAL OF MODERN MEDICINE AND PRACTICE
Vol. 4 No. 7 (Jul - 2024) EJMMP ISSN: 2795-921X

CHARACTERIZATION OF SILVER NANOPARTICLES ISOLATED FROM BACILLUS CEREUS BACTERIA AND STUDY OF THEIR EFFECTIVENESS AGAINST BIOFILMS

Mohammed aqeel abdulrazzaq, Ismaal Jmia Abas
Department of Biology, College of Education, Qurna University of Basrah, Basrah, IRAQ

Abstract: Silver nanoparticles were synthesized using the extracellular technique by utilizing the supernatant solution of Bacillus cereus bacterium, which was isolated from soil polluted with animal dung at farms located north of Basra city. The bacterial isolate demonstrated the capacity to produce silver nanoparticles, and its phenotypic and culture properties were analyzed. The study involves molecular diagnosis and characterization of silver nanoparticles through various techniques and devices. This is demonstrated by the observed color change in a reaction mixture containing 10 ml of 1 mM AgNO3 solution and 90 ml of the supernatant solution of bacteria. Specifically, the color of the reaction mixture transitions from yellow to brown, which is analyzed using a UV-visible spectrophotometer. The silver nanoparticles exhibited an absorption specifically at a wavelength of 430 nm. The EDX device achieved a purity of 70.50% for AgNPs. These silver nanoparticles were then utilized to hinder bacterial growth through the well diffusion method. Additionally, they demonstrated the capability to prevent biofilm formation in pathogenic bacterial isolates such as Pseudomonas aeruginosa, E. coli, Klebsiella pneumonia, and Staphylococcus aureus.

Keywords: biosynthesis silver nanoparticles, SEM , TEM, XRD, EDX , Bacillus cereus , Biofilm.

Introduction

The uncontrolled and unregulated use of antibiotics to treat bacterial illnesses has led to many bacteria becoming the primary cause of deadly infectious diseases [1]. The problem of bacteria developing resistance to antibiotics has motivated researchers to seek extremely effective alternatives for eradicating antibiotic-resistant bacterial species, and one of the foremost. These alternatives are nanotechnologies that strive to create materials with distinct requirements. Nanomaterials possess a minute size ranging from 1 to 100 nanometers, together with a sturdy structure and a substantial surface area relative to their size. These attributes have facilitated their utilization in several domains as antibacterial agents. The substances mentioned have properties that can combat cancer, reduce inflammation, and fight against bacterial infections [2]. Nanoparticles can be synthesized by chemical, physical, and biosynthetic techniques. Biosynthesis processes are regarded as very secure due to their ecologically benign nature, cost-effectiveness, absence of harmful byproducts, and little energy use [3]. Plant extracts, fungi, and various types of bacteria were utilized in the process of biosynthesis [4]. Bacillus cereus bacteria have been widely employed in various biological applications, particularly in the agricultural sector for producing substances that promote plant growth [5]. In this study, Bacillus cereus isolated from soil was used to synthesize silver nanoparticles, which were found to possess antibacterial properties, inhibiting bacterial growth [6]. Nanotechnology has been utilized in the medical domain to create nanoantibiotics, which are antibacterial

agents. These nanoantibiotics have demonstrated efficacy in combating infectious illnesses that exhibit resistance to numerous antibiotics [7]. Silver has a long and well-documented history of being used to cure various disorders, including eye diseases, venereal diseases, cholera, dysentery, infections, burns, and wounds [8]. Silver nanoparticles exert an impact on the bacteria constituting biofilms by traversing the channels and tunnels inside the biofilm structure. Due to their diminutive dimensions (5 nm), they possess the ability to effortlessly traverse the biofilm, subsequently attaching to the plasma membrane, infiltrating the membrane, and gaining entry into the cell. This results in altering the composition of the plasma membrane and interfering with the functioning of efflux pumps, ultimately causing the plasma membrane to collapse and resulting in the demise of the bacterial cell [9].

2- Materials and methods

2-1 : Sample collection

Samples were collected from soil contaminated with animal manure on farms north of the city of Basra. The soil was dug to a depth of 5 cm, and the soil sample was kept in a sterile plastic bottle and transported to the laboratory. 1 gram of soil was weighed and dissolved in 5 ml of distilled water in a test tube. 0.5 ml of the suspension was taken and spread on the nutrient agar medium using a cotton swab, and the plates were inoculated in the incubator at 37 °C for 24 hours [10]. When the bacterial colonies showed growth on the nutrient agar medium, single colonies were transferred to a plate. new petri in order to obtain pure colonies, then the plates were incubated in the incubator at a temperature of 37 °C for 24 hours, and their purity was confirmed by staining them with Gram dye and examining them under a microscope [11].

2-2: Diagnosis, phenotypic, and biochemical tests for bacterial isolation

The bacterial isolate isolated from the soil was identified through phenotypic examinations and biochemical tests [12]. The cultivation characteristics of the bacteria growing on the culture media were relied upon, which included the size and color of the colony, in addition to the texture and height of the colony [13].

2-3 : Molecular diagnostics

The genomic DNA was extracted using the Presto ^{TM} mini g DNA bacteria kit, which was obtained from Geneaid, and the DNA was electrophoresed [14], The polymerase chain reaction (PCR) of the DNA was performed using a master mix consisting of a group polymerase reaction and *16S rRNA* gene primers (F27) and (R1492), and the contents were transferred to special tubes and placed in the Thermometer PCR device for the purpose of performing the genomic DNA amplification process. The device was programmed as mentioned in [15].

2-4: Preparation of silver nitrate salt solution

1 mM concentration of AgNPs was prepared by dissolving 42.1 mg in 100 ml of distilled water and keeping the solution in an opaque, tightly sealed glass box to prevent oxidation [16].

2-5 : Biosynthesis of silver nanoparticles

A 250-milliliter conical flask was made, with 100 milliliters of nutritional broth medium within. The medium was inoculated with colonies of B. cereus, and the bacterial culture was cultured in a shaking incubator at a temperature of 37 °C with a shaking speed of 150 rpm for a duration of 24 hours. Following the completion of the incubation time, the bacterial culture was subjected to centrifugation at a velocity of 8000 revolutions per minute, resulting in the collection of the bacterial supernatant solution. A 10 ml aliquot of the bacteria's supernatant solution was combined with 90 ml of a solution containing silver nitrate salts at a concentration of 1 mM in a conical flask. The mixture was then kept in a shaking incubator at a temperature of 37 °C for 24 hours. After the incubation period, a change in hue was detected in the reaction mixture at a shaking speed of 150 rpm. The user's text is "[17]".

2-6: Characterization of silver nanoparticles

2-6-1: Color change

The Color change of the reaction mixture consisting of the supernatant of bacteria with the solution of silver nitrate salts is the first indication of the reduction of silver nitrate salts and the formation of silver nanoparticles [18].

2-6-2: UV-VIS Spectroscopy

The formation of silver nanoparticles was detected by knowing the optical properties of the silver nanoparticle solution using the UV-vis spectroscopy device, where the device was zeroed with the supernatant of bacteria used in reducing silver nitrate salts, and 2 ml of silver nanoparticle solution was added to the quartz tube (Cuvate), and the absorbance was measured within a wavelength of 200–1000 nm).

2-6-3 : Fourier Transmission Infrared Spectroscopy (FT-IR)

The examination was conducted to detect the active groups in the supernatant of bacteria that contributed to the reduction of AgNO3 to AgNPs within the range (450–4500 nm), where the silver nanoparticles were extracted by centrifugation of the reaction mixture and drying the extract in an electric oven at a temperature of 60° for 6 hours. The silver nanoparticle powder was mixed with Dymethial sulfoxide , and the measurement was done with an FT-IR device.

2-6-4: Scanning electron microscope and transmission electron microscopy

SEM and TEM microscopes were used to determine the shape and size of silver nanoparticles and to detect the surface nature of silver nanoparticles at a voltage of 100 kV.

2-6-5: X-ray diffraction

X-ray diffraction examination of silver nanoparticles formed to detect the crystal structure was performed by a device of the type Shimadzu 600, where silver nanoparticle powder was placed on the surface of the silicon chip and the examination was carried out.

2-6-6 : Energy Dispersive X-ray Spectroscopy (EDX)

The silver nanoparticle sample was examined by an EDX instrument to detect the of silver nanoparticles formed by the supernatant of *B. cereus* bacteria.

2-7-1 : Antibacterial activity

Four bacterial species were chosen for this study: Pseudomonas auruginosa, Escherichia coli, Klebsiella pneumonia, and Staphylococcus aureus. These bacteria were isolated from acute infections and exhibited high levels of antibiotic resistance. Four solutions of silver nanoparticles were prepared with concentrations of 25 µg/ml, 50 µg/ml, 75 µg/ml, and 100 µg/ml. The bacterial species were then activated in test tubes containing 5 ml of nutrient broth medium. Next, 0.1 ml of the bacterial culture was taken and spread onto plates containing Muller-Hinton agar medium. The plates were soaked in the medium for 10 minutes using a cotton swab. Subsequently, 6 mm diameter apertures were created in the dishes, followed by the introduction of nanosilver concentrations into the apertures. The dishes were incubated for 24 hours at a temperature of 37 °C. After the incubation period, the diameters of the dishes were measured. Suppression [19].

2-7-2 : Biofilm detection by microtiter plate

Biofilm formation was detected in bacterial species isolated from severe infections of patients hospitalized by inoculating test tubes containing 5 ml of nutrient broth medium containing a 2% glucose solution, and

150 µl of the bacterial culture was taken using a micropipette. The microtiter plate was added to the pits and was considered a positive control pit (A), and the nutrient broth medium that did not contain bacterial colonies was added to the remaining pits and was considered a negative control pit (AC). The microtiter plate was incubated in the incubator at a temperature of 37 °C for 24 hours, and after the end of the incubation period, the contents of the microtiter plate were emptied and washed with PBS.. After that, crystal violet dye at a concentration of 1% was added to the holes and left for 10 minutes. After that, the contents of the microtiter plate were emptied and washed with PBS Glacial acetic acid at a concentration of 33% was added to the holes and measured using an ELISA device, and the intensity of biofilm formation was calculated by applying the peaks shown in the ELISA device in Table 1 [20].

Table 1: Calculating the intensity of biofilm formation by comparing absorbance (A) with (AC)

$A \leq AC$	Non-biofilm forming
$AC \leq A \leq 2 * AC$	Medium biofilms
$2 * AC \leq A$	Strong biofilms

2-7-3 : The effectiveness of silver particles in inhibiting biofilm

The bacterial species were stimulated in test tubes using a 2% nutrient broth medium, and 150 µL of bacterial cultures were extracted and introduced onto microtiter plate wells. Positive control pits (A) were prepared by adding 100 µL of silver nanoparticle solution concentrations, followed by the addition of medium. The bacterial colonies in the nutrition soup were distributed to the remaining pits, serving as a negative control factor (AC). The microtiter plate was placed in the incubator and kept at a temperature of 37 °C for a duration of 24 hours. Following the completion of the incubation time, the plate's contents were removed and rinsed with PBS. Subsequently, crystal violet dye was applied to the plate, and then the contents were once again removed and washed with PBS. Subsequently, glacial acetic acid was introduced into the etching process, and its quantity was assessed using an ELISA instrument. The inhibitory potential of silver nanoparticles was then estimated by employing equation [21].

$$\text{Biofilm inhibition ratio} = \frac{\text{Negative control wavelength} - \text{positive control Wavelength}}{\text{Negative control wavelength}} \times 100$$

3: Results and discussion

3-1 : Phenotypic diagnosis and biochemical tests

B. cereus bacteria were grown on nutrient agar medium, and their colonies appeared large in size, with a waxy texture, convex, and cream in color, as in Figure 1. This is identical to what was achieved by [22]. When the cells were stained with Gram stain, it was found that they were positive for the dye and had single or double rod shapes. or in the form of chains [23]. The results of the biochemical tests showed that the *B. cereus* bacteria were positive for most tests, as shown in Table 2.

Table 2 shows the results of biochemical tests for *B. cereus* bacteria.

Bacteria	Catalase	Oxidase	Indole	Methyl red	Citrate	Urease
B. cereus	+	+	-	+	+	+

Figure 1 shows the growth of *B. cereus* bacteria colonies on nutrient agar medium, and the colonies appear with a waxy texture and cream color.

3-2: Molecular diagnostics

molecular diagnosis of *B. cereus* bacteria was performed to confirm the results of the phenotypic and cultural diagnosis, as the results of the polymerase chain reaction of the *16SrRNA* gene showed that it has a size of 1500 pb when compared to the DNA ladder, as shown in Figure 2.. The Sanker technique was used to analyze the sequencing of the amplification product. *16SrRNA* gene for the bacterial species. After conducting a BLAST search, the isolate showed an identity with the reference species in GenBank, and the sequences of the isolate were registered in the current study with the number PP475417, as in Table 3..

Table 3: Match the percentage of the current study sample with the reference sample in GenBank and the serial number of the current study sample.

%DNA Identity	Accession No.	GenBank sample	Accession NO	Present study sample
100%	PP239587.1	*B.cereus*	PP475417	*Bacillus cereus*

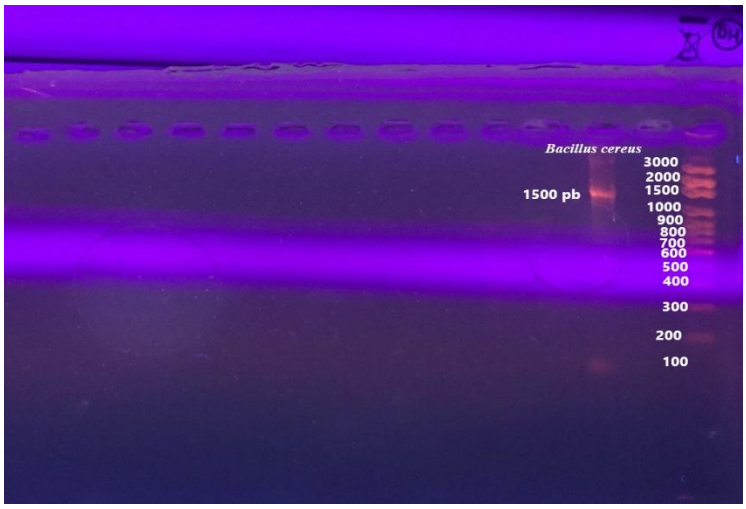

Figure 2: The resulting DNA bands after amplification with a size of 1500 pb after electrophoresis and comparing the size of the bacterial DNA with the DNA ladder

3-3 : Characterization of silver nanoparticles

3-3-1 : Color change

After the end of the incubation period of the reaction mixture consisting of 10 ml of the supernatant solution of *B. cereus* bacteria with a solution of silver nitrate salts at a concentration of 1 mM, the color of the reaction mixture changed from yellow to brown, which is the primary evidence of the formation of silver nanoparticles, as in Figure 3 The reason why the color of the reaction mixture does not appear silver is due to the phenomenon of surface plasmon resonance (SPR) that occurs in metals when the diameters of their particles reach nano-diameters [24].

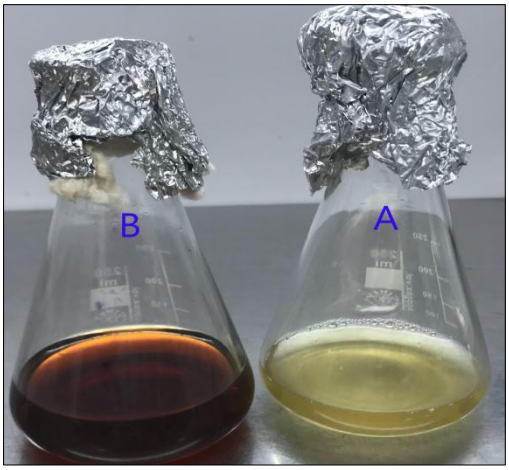

Figure 3: The color change of the reaction mixture from yellow to reddish brown, consisting of 10 ml of the supernatant solution of *B. cereus* bacteria with 90 ml of silver nitrate salt solution.

3-3-2 : UV-visible spectroscopy

UV-visible spectroscopy test was conducted on the solution of silver nanoparticles to detect the absorbance of the silver nanoparticles formed by the reduction of silver nitrate salts in the supernatant solution of *B. cereus* bacteria. The results of the test showed that the resulting silver nanoparticles had an absorption peak at a wavelength of 430 nm, as shown in Figure 4.. The results of the current study agree with [25].

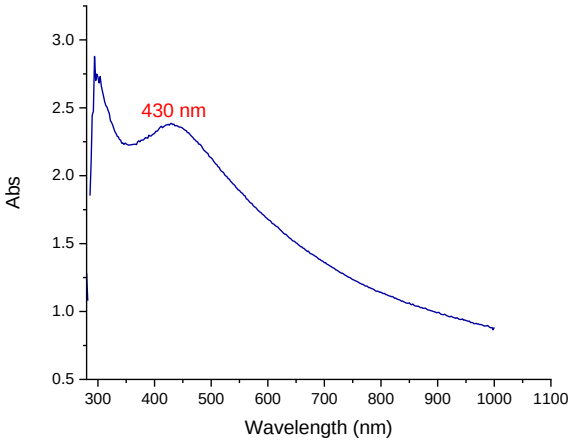

Figure 4: Absorbance of 430 nm silver nanoparticles when detected with a UV-visible spectroscopy device.

3-3-3 : Fourier-transform infrared spectroscopy (FT-IR)

The results of the FT-IR examination showed the presence of active groups associated with silver nanoparticles that contributed to the stability of the AgNPs. The results showed the presence of a peak at 3255.25 $^{cm-1}$, which indicates the O-H bond found in alcohol compounds, and a peak at 1542.77 $^{cm-1}$, which indicates the N-O bond. present in the nitro compound, and a peak of 1392.35 $^{cm-1}$, which indicates the S=O bond present in sulfonyl chloride, and another peak of 1060.66 $^{cm-1}$, which indicates the presence of S=O, which represents sulfoxide, and Figure (5) shows the apparent peaks. In the FT-IR examination, the results agreed with [26].

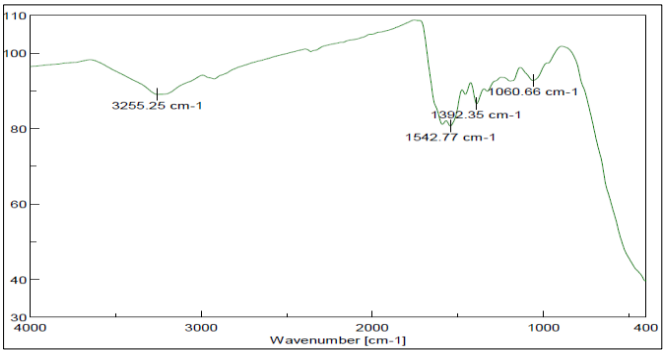

Figure 5: FT-IR examination of the visible peaks indicates the presence of active groups in the supernatant solution of *B. cereus* bacteria that coated the AgNPs and contributed to their stability.

3-3-4 : Energy Dispersive X-ray Spectroscopy (EDX)

The EDX analysis revealed that the compound formed from the synthesis of silver nanoparticles consists primarily of silver (Ag), which accounts for 70.50% of the total weight of the sample. Additionally, traces of oxygen (O), chlorine (Cl), carbon (C), silicon (Si), and phosphorus (P) were detected, which can be attributed to the presence of oxygen in the compound. The silver nanopowder underwent oxidation in the laboratory. The existence of other elements can be attributed to the remains of previously analyzed elements that were present in the same EDX instrument. These findings are in agreement with earlier research [27].

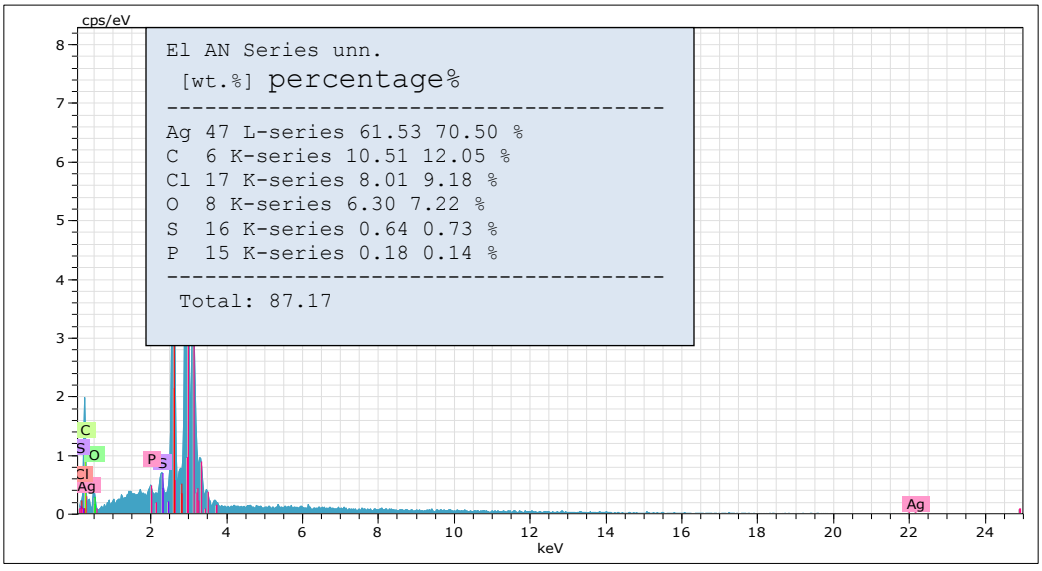

Figure 6: EDX examination showing the percentage of silver nanoparticles formed from biosynthesis by *B. cereus* bacteria and the percentage of the rest of the elements.

3-3-5 : SEM and TEM examinations

The SEM and TEM examinations showed that the silver nanoparticles formed had a semi-spherical shape, and the average size of the AgNPs in the SEM image was 32 nm. The TEM image showed that the particle sizes reached an average of 25 nm, as shown in Figure 7.. The results of the current study are compatible with [28].

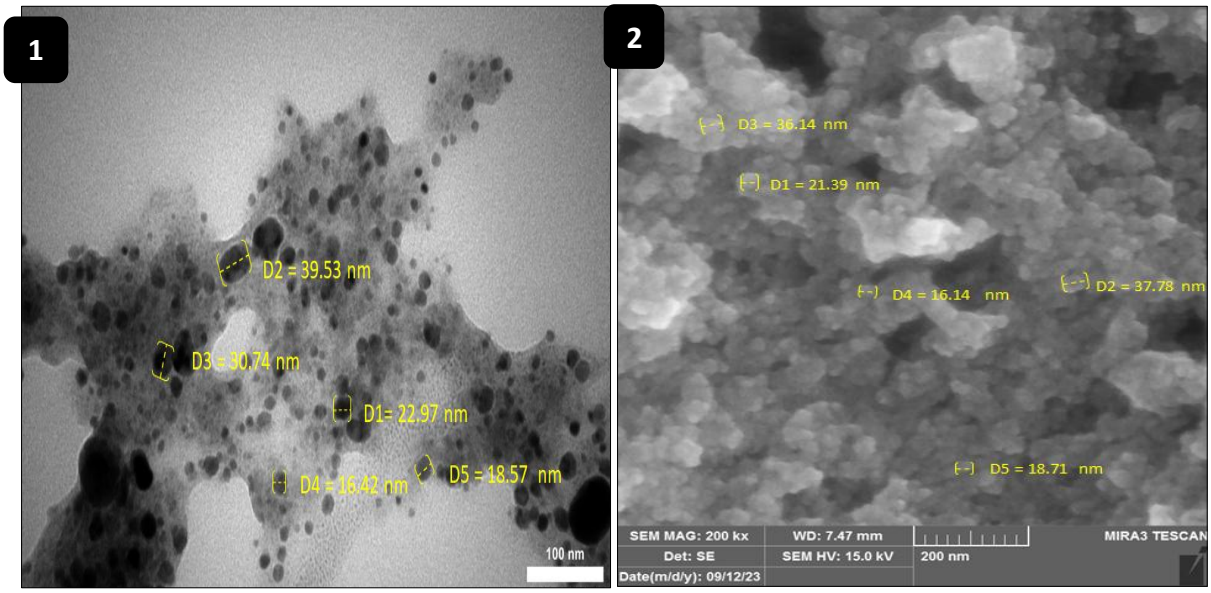

Figure (7): 1 SEM image and 2 TEM images showing the sizes of silver nanoparticles synthesized by B. cereus

3-3-6 : X-ray diffraction examination

An XRD examination was conducted to reveal the crystalline form of the formed silver nanoparticles, and the results of the examination showed the appearance of peaks (111, 220 , 311 , 222), which corresponded to 2Θ angle reflections (38.11° , 64.45 , 77.72 , 88.64°) when compared with a card. JPCDS number (00-040783). The result indicates the appearance of the silver element in a cubic crystal pattern. The other peaks (110, 111, 211, 220) were examined, which correspond to reflections at angles at 2 Θ (26.60°,32.08°, 46.23 °, 57.80°), respectively, when compared with the JCPDS card number (00-04-0793), which indicates the presence of Ag_2O as in Figure(8),) and the results were consistent with [29].

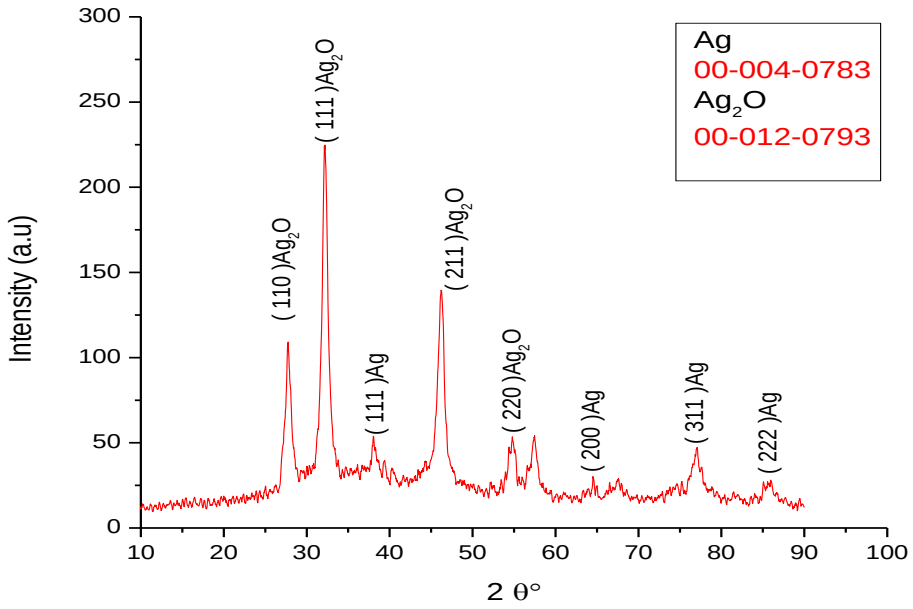

Figure 8: XRD examination of the formed silver nanoparticles and the appearance of peaks and angles that indicate the presence of Ag and Ag_2O.

3-4 : Antibacterial activity

The test results showed that when four concentrations of nanosilver (25 µg\ml, 50 µg\ml, 75 µg\ml, and 100 µg\ml) were used on four bacterial species isolated from cases of acute infections in the hospital (*P. aeruginosa*, *E. coli*, *K. pneumoniae*, and *S. aureus*), the results showed that the highest diameter of inhibition reached 23 mm on S. aureus bacteria at a concentration (100 µg\ml), and the lowest diameter of inhibition reached 12 mm on *K.pneumoniae* bacteria, and the rest of the concentrations gave varying diameters of inhibition. As in Table (4), Figure (9), and Chart (1), where the silver nanoparticles adhered to the surface of the plasma membrane and then penetrated it, they worked to stop the respiratory chain, DNA mutation, and thus the death of the bacterial cell [30].

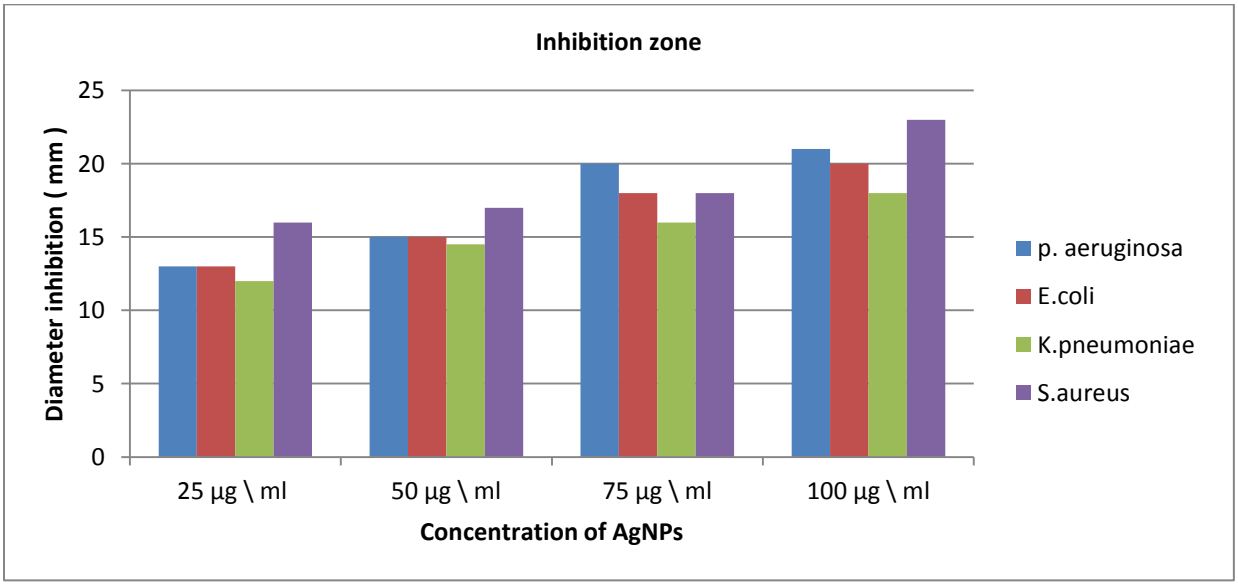

Chart 1 shows the rates of inhibition of silver nanoparticles on pathogenic bacterial species.

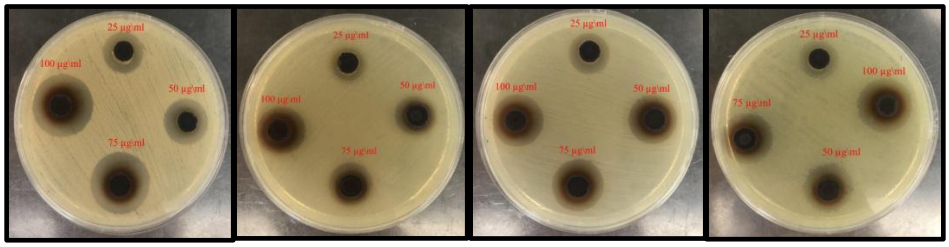

Figure 9 shows the inhibition of AgNPs on pathogenic bacterial isolates by well diffusion methods.

Table 4: Effectiveness of silver nanoparticles against the growth of pathogenic bacteria when using (25 µg\ml, 50 µg\ml, 75 µg\ml, and 100 µg\ml)

AgNPs synthesizesd from B. cereus				
Concentrations of AgNPs				Types of pathogenic bacteria
100 µg\ml	75 µg\ml	50 µg\ml	25 µg\ml	
21 mm	20 mm	15 mm	13 mm	*P. aeruginosa*
20 mm	18 mm	15 mm	13 mm	*E.coli*
18 mm	16 mm	14.50 mm	12 mm	*K.pneumoniae*
23 mm	18 mm	17 mm	16 mm	*S.aureus*

3-5 : Detection of biofilm formation

The results of the ability of the bacterial species *P. aeruginosa*, *E. coli*, *K. pneumoniae, and S. aureus* to form a biofilm were demonstrated by using a microtiter plate, where the bacteria isolated from cases of severe infections were able to form a biofilm at a high rate, as in Table 5,, and the results were consistent with [31].

Table 5: Intensity of biofilm formation in pathogenic bacterial cells by comparing the absorbance of the negative control pits (AC) with the absorbance of the positive control pits (A) when measured with the ELISA device

Biofilm intensity	Biofilm intensity calculation equation		Bacteria
Strong biofilm	$2 * 0.091 \leq 1.150$	$2 * AC \leq A$	*P. aeruginosa*
Strong biofilm	$2 * 0.088 \leq 1.090$	$2 * AC \leq A$	*E.coli*
Strong biofilm	$2 * 0.095 \leq 1.138$	$2 * AC \leq A$	*K. pneumoniae*
Strong biofilm	$2 * 0.082 \leq 1.034$	$2 * AC \leq A$	*S. aureus*

3- 6 : Effectiveness of AgNPs on biofilm inhibition

Silver nanoparticles showed a high ability to inhibit biofilm formation in bacterial cultures treated with silver nanoparticles, as the highest rate of inhibition reached 93.30% on *E. coli* bacteria when using a concentration of (100 µg/ml), while the lowest rate of inhibition reached 78.73%. On *S. aureus* bacteria when using a concentration of 25 µg/ml. Table 6 and Figure 10 show the rates of biofilm inhibition by AgNPs, as the silver nanoparticles were able to pass through the biofilm through the existing passages and channels. Inside the biofilm, it reached the bacterial cell and led to the death of the cell, forming the biofilm [32].

Table 6: Biofilm inhibition rates by using concentrations of silver nanoparticles (25 µg\ml, 50 µg\ml, 75 µg\ml, 100 µg\ml) on the bacterial species that form the biofilm

AgNPs concentrations				Types of bacteria
100 µg\ml	75 µg\ml	50 µg\ml	25 µg\ml	
91.63	89.40	88.40	86.40	*P. aeruginosa*
93.30	92.87	91.60	85.33	*E.coli*
91.87	91.10	90.13	88.67	*K. pneumoniae*
89.50	86.47	83.17	78.73	*S.aureus*

Figure 10 shows a microtiter plate showing the ability of silver nanoparticles to inhibit biofilm formation in pathogenic bacterial species.

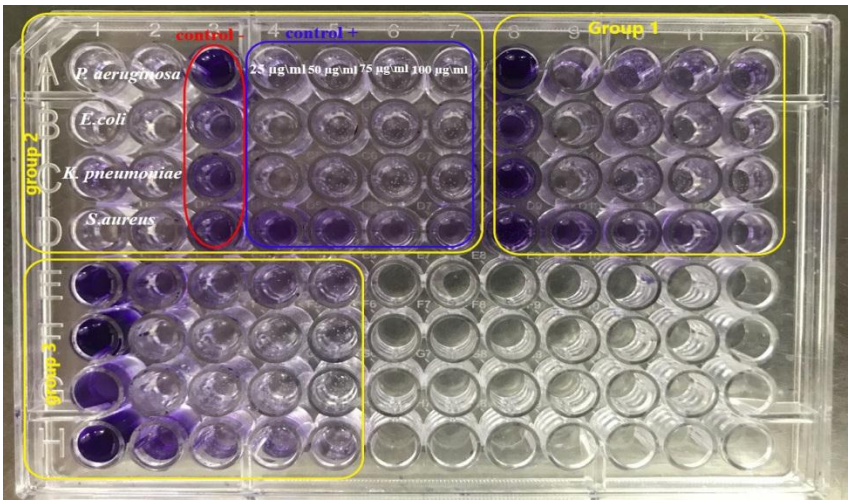

References

1. Mulani, M. S., Kamble, E. E., Kumkar, S. N., Tawre, M. S., & Pardesi, K. R. (2019). Emerging strategies to combat ESKAPE pathogens in the era of antimicrobial resistance: a review. Frontiers in microbiology, 10, 539.
2. Jalal, M., Ansari, M. A., Alzohairy, M. A., Ali, S. G., Khan, H. M., Almatroudi, A., & Siddiqui, M. I. (2019). Anticandidal activity of biosynthesized silver nanoparticles: effect on growth, cell morphology, and key virulence attributes of Candida species. International journal of nanomedicine, 4667-4679.
3. Yedurkar, S. M. M. (2016). Synthesis of Nanoparticles by Green Chemistry Process and Their Application in Surface Coatings.
4. Sulaiman, O., Salim, N., Nordin, N. A., Hashim, R., Ibrahim, M., & Sato, M. (2012). THE POTENTIAL OF OIL PALM TRUNK BIOMASS AS AN ALTERNATIVE SOURCE FOR COMPRESSED WOOD. BioResources, 7(2).
5. Mandal, A. (2015). Review on microbial xylanases and their applications. Appl Microbiol Biotechnol, 42, 45-42.

6. Silambarasan, S., & Abraham, J. (2012). Biosynthesis of silver nanoparticles using the bacteria Bacillus cereus and their antimicrobial property. Int. J. Pharm. Pharm. Sci, 4(SUPPL 1), 536-540.
7. Hajipour, M. J., Fromm, K. M., Ashkarran, A. A., de Aberasturi, D. J., de Larramendi, I. R., Rojo, T., ... & Mahmoudi, M. (2012). Antibacterial properties of nanoparticles. Trends in biotechnology, 30(10), 499-511.
8. Müller, J., & Lippert, B. (Eds.). (2023). Modern Avenues in Metal-Nucleic Acid Chemistry. CRC Press.
9. Lok, C. N., Ho, C. M., Chen, R., He, Q. Y., Yu, W. Y., Sun, H., ... & Che, C. M. (2007). Silver nanoparticles: partial oxidation and antibacterial activities. JBIC Journal of Biological Inorganic Chemistry, 12, 527-534.
10. Mulamattathil, S. G., Bezuidenhout, C., Mbewe, M., & Ateba, C. N. (2014). Isolation of environmental bacteria from surface and drinking water in Mafikeng, South Africa, and characterization using their antibiotic resistance profiles. Journal of pathogens, 2014(1), 371208.
11. Patowary, K., Patowary, R., Kalita, M. C., & Deka, S. (2017). Characterization of biosurfactant produced during degradation of hydrocarbons using crude oil as sole source of carbon. Frontiers in microbiology, 8, 279.
12. Almansoory, A. F., Talal, A., Al-Yousif, N. A., & Hazaimeh, M. (2019). Isolation and identification of microbial species for hydrocarbon degradation in contaminated soil and water.
13. Wanger, A., Chavez, V., Huang, R., Wahed, A., Dasgupta, A., & Actor, J. K. (2017). Microbiology and molecular diagnosis in pathology: a comprehensive review for board preparation, certification and clinical practice.
14. Sambrook, J. (2001). Molecular cloning: a laboratory manual/Joseph Sambrook, David W. Russell. Q. Rev. Biol, 76, 348-349.
15. Maleki, D., Jahromy, S. H., Karizi, S. Z., & Eslami, P. (2016). The prevalence of acrA and acrB genes among multiple-drug resistant uropathogenic Escherichia coli isolated from patients with UTI in Milad Hospital, Tehran. Avicenna Journal of Clinical Microbiology and Infection, 4(1), 39785-39785.
16. Nagati, V. B., Alwala, J., Koyyati, R., Donda, M. R., Banala, R., & Padigya, P. R. M. (2012). Green synthesis of plant-mediated silver nanoparticles using Withania somnifera leaf extract and evaluation of their antimicrobial activity. Asian Pac J Trop Biomed, 2, 1-5.
17. Nikhil, A., Kolte, N. A., Tumane, P. M., & Wasnik, D. D. (2017). Extracellular biosynthesis and characterization of silver nanoparticles by using Bacillus cereus gad 20 and their antibacterial potential against E. coli and S. aureus. Int J Curr Res, 9, 61849-56.
18. Singh, R., Wagh, P., Wadhwani, S., Gaidhani, S., Kumbhar, A., Bellare, J., & Chopade, B. A. (2013). Synthesis, optimization, and characterization of silver nanoparticles from Acinetobacter calcoaceticus and their enhanced antibacterial activity when combined with antibiotics. International journal of nanomedicine, 4277-4290.
19. Balouiri, M., Sadiki, M., & Ibnsouda, S. K. (2016). Methods for in vitro evaluating antimicrobial activity: A review. Journal of pharmaceutical analysis, 6(2), 71-79.
20. Tang, J., Kang, M., Chen, H., Shi, X., Zhou, R., Chen, J., & Du, Y. (2011). The staphylococcal nuclease prevents biofilm formation in Staphylococcus aureus and other biofilm-forming bacteria. Science China Life Sciences, 54, 863-869.

21. Namasivayam, S. K. R., Preethi, M., Bharani, A., Robin, G., & Latha, B. (2012). Biofilm inhibitory effect of silver nanoparticles coated catheter against Staphylococcus aureus and evaluation of its synergistic effects with antibiotics. Int J Biol Pharm Res, 3(2), 259-265.
22. Ouertani, A., Chaabouni, I., Mosbah, A., Long, J., Barakat, M., Mansuelle, P., ... & Cherif, A. (2018). Two new secreted proteases generate a casein-derived antimicrobial peptide in Bacillus cereus food born isolate leading to bacterial competition in milk. Frontiers in microbiology, 9, 1148.
23. Batt, C. A. (2000). Bacillus cereus. Encyclopedia of food microbiology, 1, 119-149.
24. Saravanan, M., Barik, S. K., MubarakAli, D., Prakash, P., & Pugazhendhi, A. (2018). Synthesis of silver nanoparticles from Bacillus brevis (NCIM 2533) and their antibacterial activity against pathogenic bacteria. Microbial pathogenesis, 116, 221-226.
25. Chaudhari, P. R., Masurkar, S. A., Shidore, V. B., & Kamble, S. P. (2012). Effect of biosynthesized silver nanoparticles on Staphylococcus aureus biofilm quenching and prevention of biofilm formation. Nano-Micro Letters, 4, 34-39.
26. Pavia, D. L., Lampman, G. M., Kriz, G. S., & Vyvyan, J. R. (2015). Introduction to spectroscopy.
27. Kalimuthu, K., Babu, R. S., Venkataraman, D., Bilal, M., & Gurunathan, S. (2008). Biosynthesis of silver nanocrystals by Bacillus licheniformis. Colloids and surfaces B: Biointerfaces, 65(1), 150-153.
28. Das, V. L., Thomas, R., Varghese, R. T., Soniya, E. V., Mathew, J., & Radhakrishnan, E. K. (2014). Extracellular synthesis of silver nanoparticles by the Bacillus strain CS 11 isolated from industrialized area. 3 Biotech, 4, 121-126.
29. Abdalameer, N. K., Khalaph, K. A., & Ali, E. M. (2021). Ag/AgO nanoparticles: Green synthesis and investigation of their bacterial inhibition effects. Materials Today: Proceedings, 45, 5788-5792.
30. Nasiri, A., Gharebagh, R. A., Nojoumi, S. A., Akbarizadeh, M., Harirchi, S., Arefnezhad, M., ... & Sargazi, A. (2016). Evaluation of the antimicrobial activity of silver nanoparticles on antibiotic-resistant Pseudomonas aeruginosa. International Journal of Basic Science in Medicine, 1(1), 25-28.
31. Slížová, M., Nemcová, R., Mad'Ar, M., Hadryová, J., Gancarčíková, S., Popper, M., & Pistl, J. (2015). Analysis of biofilm formation by intestinal lactobacilli. Canadian journal of microbiology, 61(6), 437-446.
32. Gupta, D., Singh, A., & Khan, A. U. (2017). Nanoparticles as efflux pump and biofilm inhibitor to rejuvenate bactericidal effect of conventional antibiotics. Nanoscale research letters, 12, 1-6.